Facile Solvothermal Preparation of Monodisperse Gold Nanoparticles and Their Engineered Assembly of Ferritin-Gold Nanoclusters

ARTICLE *in* LANGMUIR · NOVEMBER 2013

Impact Factor: 4.46 · DOI: 10.1021/la403888f · Source: PubMed

8 AUTHORS, INCLUDING:

Zoran Slobodan Stojanovic
Serbian Academy of Sciences and Arts
17 PUBLICATIONS **160** CITATIONS
SEE PROFILE

Hyung-Seop Han
Korea Institute of Science and Technology
36 PUBLICATIONS **224** CITATIONS
SEE PROFILE

Kwan Hyi Lee
Korea Institute of Science and Technology
39 PUBLICATIONS **316** CITATIONS
SEE PROFILE

Dragan P. Uskoković
Serbian Academy of Sciences and Arts
273 PUBLICATIONS **2,858** CITATIONS
SEE PROFILE

Langmuir

Article

pubs.acs.org/Langmuir

Facile Solvothermal Preparation of Monodisperse Gold Nanoparticles and Their Engineered Assembly of Ferritin−Gold Nanoclusters

Jonghoon Choi,[†,‡] Sungwook Park,[§] Zoran Stojanović,[∥] Hyung-Seop Han,[§] Jongwook Lee,[§] Hyun Kwang Seok,[§] Dragan Uskoković,[∥] and Kwan Hyi Lee*[,§]

[†]Executive Office, Institute of Research Strategy and Development (IRSD), Seoul 137-781, Republic of Korea

[‡]Department of Bionano Engineering, Hanyang University, Ansan 426-791, Republic of Korea

[§]Center for Biomaterials, Biomedical Research Institute, Korea Institute of Science and Technology, Seoul 136-791, Republic of Korea

[∥]Center for Fine Particles Processing and Nanotechnologies, Institute of Technical Sciences of the Serbian Academy of Sciences and Arts, Knez-Mihailova 35, 11000 Belgrade, Republic of Serbia

Supporting Information

ABSTRACT: Herein, we report a quick and simple synthesis of water-soluble gold nanoparticles using a $HAuCl_4$ and oleylamine mixture. Oleylamine serves as a reduction agent as well as a stabilizer for nanoparticle surfaces. The particle sizes can be adjusted by modulating reaction temperature and time. Solvothermal reduction of $HAuCl_4$ with oleylamine can be confirmed by measuring the product in Fourier transform infrared (FTIR) spectroscopy. The plasmon band shifting from yellow to red confirms a nanosized particle formation. Amide bonds on the surface of the nanoparticles formed hydrogen bonds with one another, resulting in a hydrophobic monolayer. Particles dispersed well in nonpolar organic solvents, such as in hexane or toluene, by brief sonication. Next, we demonstrated the transfer of gold nanoparticles into water by lipid capsulation using 1-myristoyl-2-hydroxy-*sn*-glycero-3-phosphocholine (MHPC), 1,2-distearoyl-*sn*-glycero-3-phosphoethanolamine-*N*-(methoxy polyethylene glycol)-2000 (DPPE-PEG2k), and 1,2-dioleoyl-*sn*-glycero-3-*N*-{5-amino-1-carboxypentyl}iminodiacetic acid succinyl nickel salt [DGS-NTA(Ni)]. The particle concentration can be obtained using an absorbance in ultraviolet−visible (UV−vis) spectra (at 420 nm). Instrumental analyses using transmission electron microscopy (TEM), energy-dispersive X-ray (EDX) analysis, dynamic light scattering (DLS), and FTIR confirmed successful production of gold nanoparticles and fair solubility in water. Prepared gold particles were selectively clustered via engineered ferritin nanocages that provide multiple conjugation moieties. A total of 5−6 gold nanoparticles were clustered on a single ferritin nanocage confirmed in TEM. Reported solvothermal synthesis and preparation of gold nanoclusters may serve as an efficient, alternate way of preparing water-soluble gold nanoparticles, which can be used in a wide variety of biomedical applications.

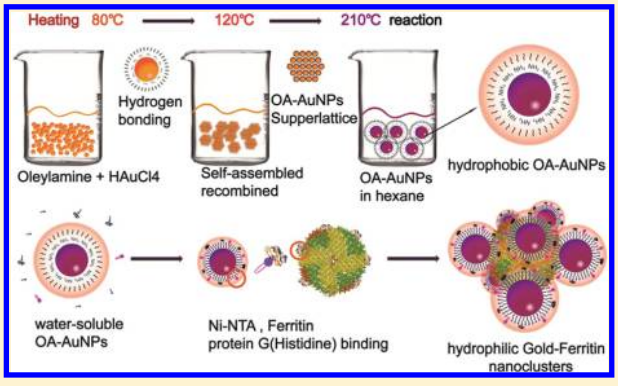

INTRODUCTION

Nanosized particles have unique chemical and physical properties when compared to bulk materials.[1] This is due to an increase in surface area and the effect of quantum confinement in the nanometer regime. Gold nanoparticles possess their unique optical, physical, and chemical properties because of their small size.[2] Well-known properties, such as surface plasmon resonance (SPR), surface-enhanced Raman scattering (SERS), and nonlinear optical (NLO) properties, are all attributed to their nanometer sizes. In addition, electronic properties, high stability, and biological compatibility of gold nanoparticles have also received a great amount of attention because of their potential biomedical applications in biosensing, probing, and targeting in tumor treatment.[3−6] Biosensors prepared with nanoconstructs have fast response and good sensitivity and specificity that allow for reduction in cost and time for the analysis. Furthermore, small sizes of nanoparticles minimize the damage to the cell during optical staining or biomarker tagging as well as during the delivery of biomolecules/drugs to the target cell/tissue/organ.[7−9] Optical properties of the gold nanoparticle allow for efficient detection

Received: October 8, 2013
Revised: November 21, 2013
Published: November 27, 2013

of DNA molecules by conjugation with the target DNA strand that results in the plasmon shift.[10,11]

There are several reported methods to synthesize gold nanoparticles. Two of the most popular methods are based on condensation and reduction.[12−14] The condensation-based method assembles particles and grows them on a cooled template using the condensation of gold ions, while the reduction-based method applies reduction of metal ions using proper reducing agents that can produce nanosized gold particles.

Previously reported synthesis methods, such as the Turkevich approach, include sodium citrate as a reducing agent, leading to a long reaction time. In this work, we adapted the Brust method to reduce the reaction time and produce monodisperse gold nanoparticles in a more effective manner. In the modified method in our report, we prepare the gold particles with $HAuCl_4$, thus eliminating the requirement of organic solvents, such as toluene or chloroform, in the reaction. The only solute, oleylamine, is involved in the benign reaction. The product of this simple reaction would be nanosized gold particles with a hydrophobic surface that disperse well in nonpolar solvents. Because the biocompatibility of nanoparticles and biomedical applications requires particles to be water-soluble, a wide variety of approaches to modify the surface chemistry of particles has been reported.[15−21] Three different lipids, 1-myristoyl-2-hydroxy-*sn*-glycero-3-phosphocholine (MHPC), 1,2-distearoyl-*sn*-glycero-3-phosphoethanolamine-*N*-(methoxy polyethylene glycol)-2000 (DPPE-PEG2k), and 1,2-dioleoyl-*sn*-glycero-3-*N*-{5-amino-1-carboxypentyl}-iminodiacetic acid succinyl nickel salt [DGS-NTA(Ni)], are used in the reaction process to help functionalize and stabilize the surface of particles in water.[19−21] Hydrophobic heads of lipids bind to the particles and leave the hydrophilic tails free to promote the particles to be water-soluble. The addition of DGS-NTA(Ni) lipid in the reaction provides functional moiety to the particles that can specifically bind to the histidine of the target protein. We demonstrate here the conjugation of multiple gold nanoparticles to the ferritin nanocage for enhanced optical properties per each nanoconstruct. A ferritin nanocage consists of 24 subunits that are self-assembled into a spherical structure, and the spherical structure allows for both antibody immobilization and gold particle tagging.[19] Because each vector has both protein-G- and histidine-expressing promoter regions, transfected *Escherichia coli* produces a dual-functioning ferritin nanocage. By conjugating gold nanoparticles to a ferritin nanocage, we expect that the ferritin nanocage will use the gold nanoparticles to target the biomolecules of our choice and enhance their limit of detection. The reported method is not only simple and cost-effective but capable of providing monodisperse, functional gold nanoparticles that can be characterized in transmission electron microscopy (TEM), dynamic light scattering (DLS), Fourier transform infrared (FTIR) spectroscopy, and ultraviolet−visible (UV−vis) spectrometer. It is expected that this alternative solvothermal method of preparing a gold nanoparticle may become an efficient protocol that can be routinely performed to produce a mass amount of gold nanoparticles for biomedical applications. Furthermore, the described approach using gold−ferritin nanoclusters may help extend the lower limits of detection for biomolecules.

MATERIALS AND METHODS

Reagents. All reagents, including gold(III) chloride solution ($HAuCl_4$, 99.99% trace metals basis) and oleylamine (technical grade, 70%), were purchased from Sigma-Aldrich. MHPC, DPPE-PEG2k, and DGS-NTA(Ni) lipids are obtained from Avanti, Inc.

Synthesis of Oleylamine-Protected Gold Nanoparticles. In a typical procedure, 50 μL of 30 wt % $HAuCl_4$ in HCl solution (17 wt % Au) was added to 1.5 mL of oleylamine at 60 °C in a 25 mL beaker on a hot plate. The mixture was magnetically stirred for 15 min to homogenize and evaporate water. The temperature was increased to 120 °C on a hot plate, stirred for 30 min, raised to 210 °C, and stirred for another 1 h. To homogenize the particle size, the samples were slowly cooled. Then, samples were put in 15 mL of ethanol and then centrifuged at 5000 rpm for 10 min. The supernatant was discarded and redispersed in 8 mL of ethanol before sonication for 30 s. The samples were washed 3 times. After the final washing step, the leftover liquid was decanted and precipitated samples were left to dry for 3 h. Next, dried samples were redispersed in 5 mL of hexane. The samples were stored in an opaque vial for further characterization and manipulation.

Surface Modification of Gold Nanoparticles. The concentration of gold nanoparticles dispersed in hexane can be calculated with the absorbance peak (at 420 nm) from a UV−vis spectra absorbance. A 10 times higher concentration of MHPC, DPPE-PEG2k, and DGS-NTA(Ni) lipid was added to the samples to let them dissolve in water. A total of 70 μL of gold nanoparticles and lipids [80% MHPC, 15% DPPE-PEG2k, and 5% DGS-NTA(Ni)] were premixed and then dropped into water while heating the vessel, which evaporated the residual hexane in the solution. The mixed solution was slowly added by pipetting into a 5 mL beaker on a hot plate at maximum revolutions per minute for 1 min. Next, the beaker was sonicated for 1 min and heated at 90 °C on 1150 (maximum) rpm for 1 h to evaporate all solvents besides water. Again, the beaker was sonicated for 30 min, and the leftover solvent of the beaker was transferred to microtubes before centrifugation at 10000*g* for 10 min. The supernatant was transferred to a syringe and filtered through a 0.2 μm syringe filter. The filtered sample was collected in a 15 mL tube, and then the particles were encapsulated by the lipids, promoting the surface to become hydrophilic. The DLS measurement of the particles confirms the degree of encapsulation and size distribution.

Clustering Gold Nanoparticles around the Ferritin Nanocage. Synthesized gold nanoparticles in hexane were dried and mixed with excess amounts of MHPC, DPPE-PEG2k, and DGS-NTA(Ni). Next, the solution was slowly dropped into 90 °C water and mixed for 1 min before sonication. After 1 h of reaction, organic solvent in the solution was evaporated and leftover solution was centrifuged (10 min at 10000*g*) to obtain precipitates. The concentration of gold particles in the filtered supernatants was measured in DLS and absorption spectra before being mixed with ferritin nanocages. Protein G and histidine were expressed on the ferritin surface via polymerase chain reaction (PCR) and ligation. Restriction enzymes, *Nde*I and *Bam*HI were inserted into each end of the ferritin vector. In addition, histidine-included protein G is also genetically engineered to carry restriction enzymes, *Bam*HI and *Xho*I. Using these two DNA strand ligations, protein G and histidine were successfully engineered.

The sequence was confirmed by inserting these DNA strands into a T vector, and genes were expressed by transferring them to DH5α (*E. coli*). Overexpressed ferritin and protein G genes were inserted into pET vector and transfected BL21 (*E. coli*) to produce self-assembled ferritin nanocages. After 1 h of reaction of ferritin nanocages and lipid-functionalized gold nanoparticles, the products were washed with phosphate-buffered saline (PBS) 3 times and centrifuged.

Particle Characterization. Absorption spectra of gold nanoparticles were taken using the UV−vis spectrometer (TECAN), and exported data were drawn in Excel. The DLS measurement of nanoparticles was made using the ZetaSizer Nano-ZS (Malvern), and TEM images were taken using the FEI G2 F20 Cryo electron microscope (Technai). To prepare particle samples for TEM, gold particles were diluted to $^1/_{20}$ and 5 μL of the diluted samples was

dx.doi.org/10.1021/la403888f | *Langmuir* 2013, 29, 15698−15703

Scheme 1. Solvothermal Synthesis of Gold Nanoparticles and Surface Exchange with Lipids for Water Solubility: (A) Stepwise Process of Synthesizing Gold Nanoparticles and Encapsulating the Particles with a Mixture of Lipids and (B) Application of Gold Nanoparticles to Tag Ferritin Nanocages

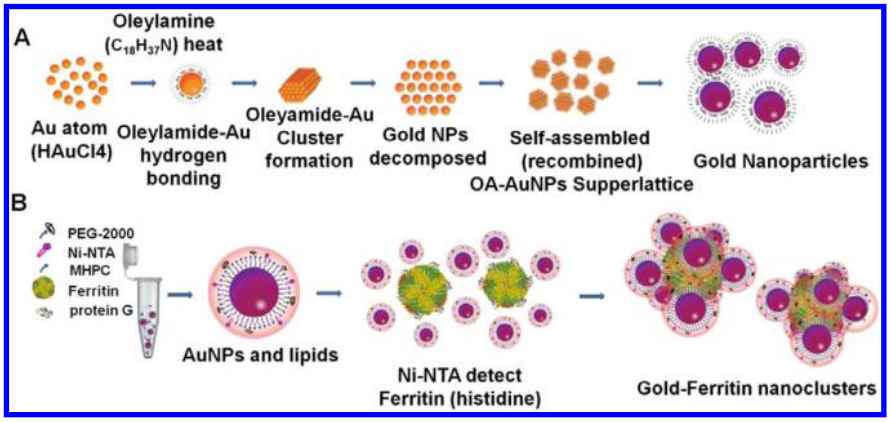

loaded to a TEM grid. For the DLS measurement, 1 mL particle samples in hexane were diluted to $^{1}/_{20}$, while water-soluble particles were directly measured in the cuvette.

FTIR spectra were measured in Thermo Mattson Model Infinity. The particle samples spotted on an IR card (Teflon) were dried and delivered to the machine. After the measurement, only signal-to-noise ratios over 100 000:1 root mean square (rms) and resolutions greater than 0.7 cm^{-1} were analyzed.

RESULTS AND DISCUSSION

Scheme 1 depicts the entire process of preparing water-soluble, monodisperse gold nanoparticles. The originality of our synthesis method based on the Brust approach is that we did not use organic solvent, such as toluene or chloroform. Instead, oleylamine, which stabilizes the surface and reduces gold ions, was used. The successful demonstration of oleylamine as a reducing agent for gold nanoparticle synthesis is quite noteworthy. Simple elevation of the temperature from 60 to 120 and 210 °C in a reaction beaker containing $HAuCl_4$ and oleylamine is all that is needed for the process. Leftover oleylamine is washed with excess methanol using continuous sonication and centrifugation. Precipitated samples (OA-GNP) can be stored in nonpolar organic solvent (e.g., hexane).

The progress of synthesized nanoparticles can be confirmed by the plasmonic shift that is due to the electrons in the conduction band interacting with the electromagnetic field. In the case of Au, Ag, and Cu materials, nanosized particles strongly absorb the visible light. UV–vis spectra of gold nanoparticles display this strong absorption at around 530 nm (Figure 1). Because the size and shape of the particles determine the absorption wavelength and coefficient, the absorption of gold nanoparticles smaller than 2 nm is weak and dependent upon the diameter. Shifting of the plasmonic peak was observed (the color of the solution changes from yellow to red) as the size of the particle became larger.

Figure 1 depicts the unique absorption peak of gold nanoparticles at 530 nm, which confirms the synthesized nanoparticles. The concentration of the nanoparticles can be calculated from the Beer–Lambert law ($A = \varepsilon bC$) using the molar absorptivity and the absorbance measured in UV–vis spectra, where A is the absorbance, b is the path length of the sample (cm), C is the concentration of the compound in solution (mol/L), and ε is the molar absorptivity (L mol^{-1} cm^{-1}). The molar absorptivity is calculated from the measured diameters of nanoparticles in DLS (Figure 2) and plugged into the Beer–Lambert equation that resulted in ~50 mg/mL per single experiment.

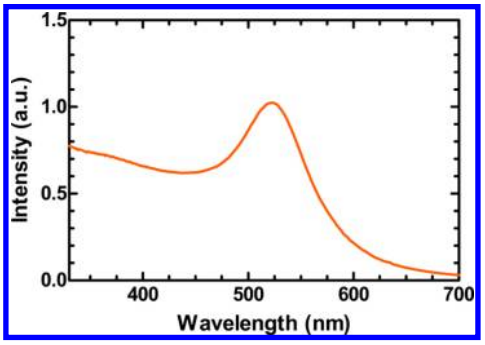

Figure 1. Representative UV–vis absorption spectrum of $HAuCl_4$ originated from gold nanoparticles in hexane.

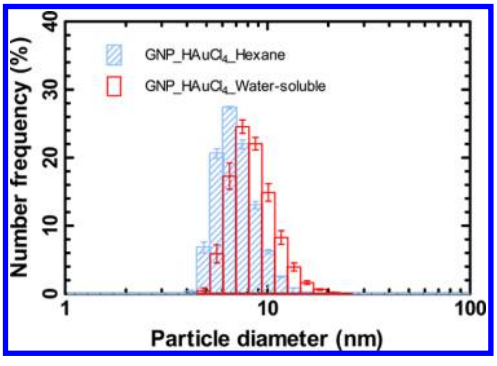

Figure 2. Representative DLS size distribution histograms of $HAuCl_4$-originated gold nanoparticles in hexane (blue) and water (red).

The mean diameter of water-soluble nanoparticles estimated from the DLS measurement is slightly increased from 7.2 to 9 nm because of lipid encapsulation. However, the size distribution histograms are similar between each particle, indicating that the gold particles are evenly coated with lipids and well-dispersed in water. TEM analysis of gold particles also confirmed the average diameter of nanoparticles (Figure 3; mean diameters = 7–9 nm). The factors controlling the mean diameter of synthesized gold nanoparticles would be the amount of oleylamine in the reaction or the reaction temperature. Previous reports summarizes the effect of a higher

dx.doi.org/10.1021/la403888f | Langmuir 2013, 29, 15698–15703

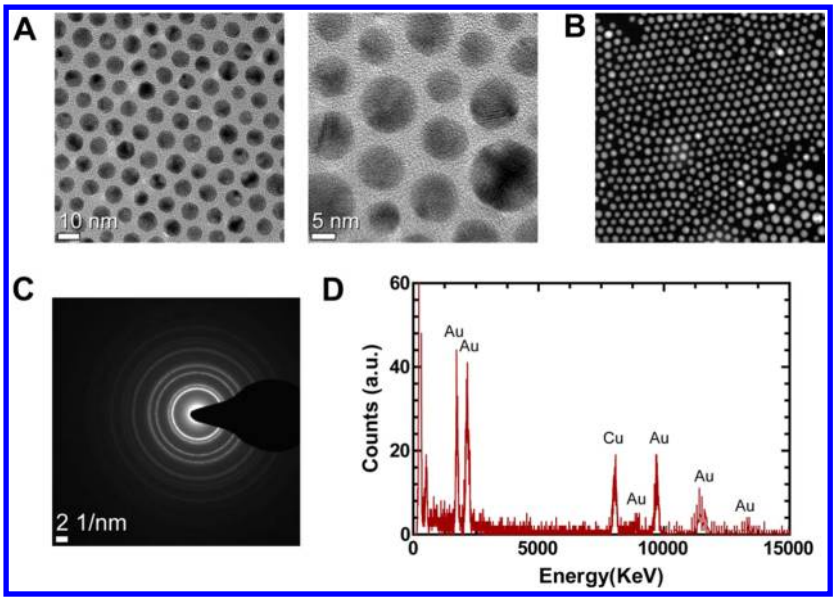

Figure 3. Characterization of the synthesized gold nanoparticles. (A) TEM analyses of nanoparticles show their mean diameter at around 7−9 nm depending upon the surface modification. (B) Representative scanning TEM (STEM) image of gold particles confirms monodisperse and spherical gold nanoparticles. (C) Crystallographic analysis of gold nanoparticles in panel A shows unique nanocrystalline structures. (D) Energy-dispersive X-ray (EDX) analysis of gold nanoparticles shows their signature peaks.

concentration of oleylamine in the reaction that results in the narrow size distribution of gold nanoparticles.[22−24] Also, the raised reaction temperature accelerates the reduction of gold ions, which are efficiently protected by the amine molecule.

Because particles in the organic solvent are not desirable for *in vitro* or *in vivo* applications, they were treated with lipids to become water-soluble. Our approach includes a use of the lipid mixture, MHPC, DPPE-PEG2k, and DGS-NTA(Ni), to obtain hydrophilic moiety and target specificity for further functionalization. A total of 80% of the lipid mixture is MHPC that has hydrophilic heads and hydrophobic tails. The hydrophobic tails interact with hydrophobic gold particles and leave hydrophilic heads free on the surface. Because of this amphiphilic nature of the lipid, particles become water-soluble. DPPE-PEG2k takes 15% of the mixture and helps to stabilize the surface structure. The last 5% is made of DGS-NTA(Ni) that provides conjugation moiety to the particles.[19−21] NTA(Ni) specifically binds to histidine that helps to target ferritin nanocages via their Ni−NTA and histidine affinity (Scheme 1B). A comparison of FTIR spectra of oleylamine and gold nanoparticle displayed a specific peak shift because of a particle formation (Figure 4).

FTIR spectra characterize the kind of bonds and functional groups. Because molecules have their own vibrational energy, continuous excitation of molecules with IR laser scanning would promote absorption at the specific wavelength. This helps to predict the molecular structure and surface chemistry of sample molecules based on *cis*−*trans* isomerism, hydrogen bonding, or chelation. Specific IR bands of oleylamine were observed at around 3500−3200 cm^{-1} for N−H stretch, at 3100−2800 cm^{-1} for C−H stretch, at 1563 cm^{-1} for N−H bending, at 1500−1300 cm^{-1} for C−H bending, at 1100−1050 cm^{-1} for weak C−N stretch, and at around 3380−3250 cm^{-1} for N−H hydrogen bonding (Figure 4). Oleylamine in the reaction reduces amines on particles to amides, which is confirmed in FTIR spectra. The most significant difference in the FTIR spectra would be the shift of vibration bands from 1570 to 1648 cm^{-1}, which is from amides. This is due to a chemical change of amines to amides, while oleylamine reduces

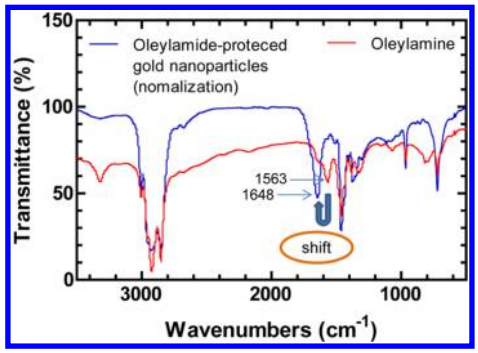

Figure 4. FTIR spectra of gold nanoparticles. The blue line is the spectrum of oleylamide protecting the gold nanoparticles (normalized), and the red line is that of oleylamine itself. Synthesized gold nanoparticles have their unique peak at around 1646 cm^{-1}, which originated from vibrational amide groups in Au.

Au(3) to Au(1) or Au(0), which confirms a well-modified surface of nanoparticles with water-solubilizing lipids.

The successful conjugation of multiple gold nanoparticles to the ferritin nanocage is illustrated in Figure 5. To form gold−ferritin nanoclusters, Ni ions on the surface of the gold nanoparticles interact with histidine residues on protein G expressed on the surface of ferritin. The three lipids modified the surface of synthesized gold nanoparticles [MHPC, DPPE-PEG2k, and DGS-NTA(Ni)]. They stabilize and act to interact with histidine groups on protein G. The water-solubilized gold−ferritin nanoclusters exhibit minimal aggregation, 3−5 gold particles per ferritin nanocage, and are well-dispersed with an average diameter of 20.5 nm, as shown in Figure 5. The size of clusters depends upon the ratio of ferritin and gold nanoparticles in the reaction. The increased amount of gold nanoparticles would bring higher opportunity for them to conjugate with ferritins, resulting in the increased diameter of clusters. This may also, however, increase the chance for gold nanoparticles aggregated with each other when they do not

dx.doi.org/10.1021/la403888f | *Langmuir* 2013, 29, 15698−15703

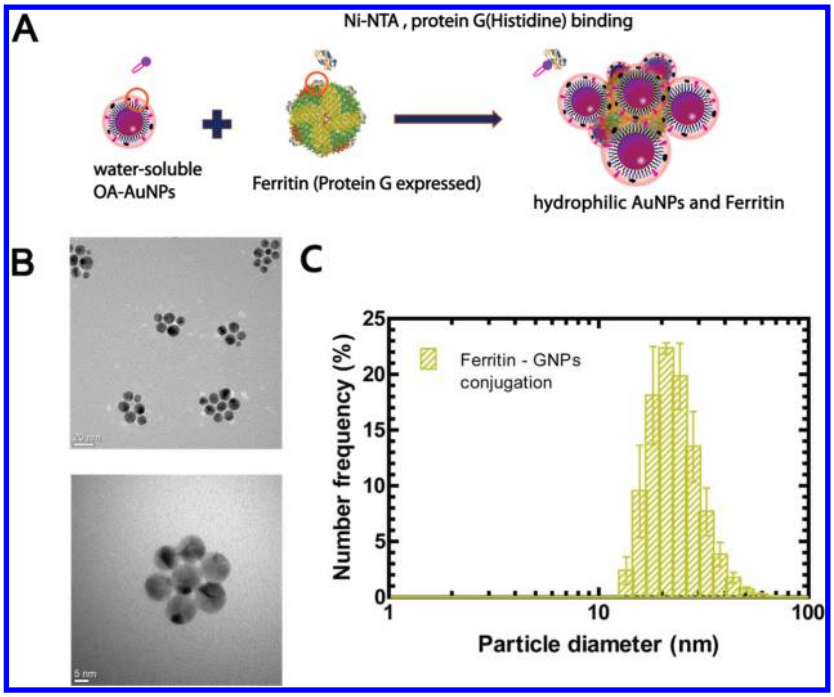

Figure 5. Characterization of gold–ferritin nanoclusters. (A) Gold nanoparticles are clustered around ferritin nanocages via NTA(Ni) and histine binding. (B) Mean size of water-solubilized gold–ferritin nanoclusters is around 20.5 nm, measured using ImageJ on several TEM images. (C) DLS measurements verify the size distribution profile of water-solubilized gold–ferritin nanoclusters.

surround the ferritin particles. It is noted that the size of gold nanoparticles would also affect the total diameter of clusters.

CONCLUSION

In this work, we presented in detail how a solvothermal synthesis approach could be used to prepare the water-soluble, monodisperse gold nanoparticles simply with oleylamine and $HAuCl_4$. The addition of oleylamine to the reaction promoted monodisperse, hydrophobic, and well-characterized small (~7 nm) gold nanoparticles. UV–vis, TEM, and DLS analyses confirm the size and monodispersity of nanoparticles, and the lipid functionalization of synthesized nanoparticles resulted in water-soluble gold nanoparticles. Multiple gold nanoparticles were successfully conjugated to a ferritin nanocage via a genetically engineered, bioconjugation strategy. Reported water-soluble gold nanoparticles have great potential in biomedical applications, such as protein tagging (e.g., ferritin nanocage), signal-amplified CT contrast agents, and SERS.

ASSOCIATED CONTENT

Supporting Information

Discussion on the characteristics of solvothermally synthesized gold nanoparticles reported in different literature compared to particles in this work. This material is available free of charge via the Internet at http://pubs.acs.org.

AUTHOR INFORMATION

Corresponding Author

*Telephone: +82-2-958-6840. Fax: +82-2-958-6629. E-mail: kwanhyi@kist.re.kr.

Notes

The authors declare no competing financial interest.

ACKNOWLEDGMENTS

This work is supported by Korea Institute of Science and Technology (KIST) (CTP Program 2V03130 and K-GRL Program 2Z03720) and a National Research Foundation of Korea (NRF) grant funded by the Korea government (MSIP) (2008-0061891).

ABBREVIATIONS USED

SPR, surface plasmon resonance; SERS, surface-enhanced Raman scattering; NLO, nonlinear optical; MHPC, 1-myristoyl-2-hydroxy-*sn*-glycero-phosphocholine; DPPE-PEG2k, 1,2-distearoyl-*sn*-glycero-3-phosphoethanolamine-*N*-(methoxy polyethylene glycol)-2000; DGS-NTA(Ni), 1,2-dioleoyl-*sn*-glycero-3-*N*-{5-amino-1-carboxypentyl}-iminodiacetic acid succinyl nickel salt; DLS, dynamic light scattering; TEM, transmission electron microscopy; STEM, scanning TEM; EDX, energy-dispersive X-ray

REFERENCES

(1) Shenhar, R.; Rotello, V. M. Nanoparticles: Scaffolds and building blocks. *Acc. Chem. Res.* **2003**, *36* (7), 549–561.

(2) Daniel, M. C.; Astruc, D. Gold nanoparticles: Assembly, supramolecular chemistry, quantum-size-related properties, and applications toward biology, catalysis, and nanotechnology. *Chem. Rev.* **2004**, *104* (1), 293–346.

(3) Indrasekara, A. S.; Paladini, B. J.; Naczynski, D. J.; Starovoytov, V.; Moghe, P. V.; Fabris, L. Dimeric gold nanoparticle assemblies as tags for SERS-based cancer detection. *Adv. Healthcare Mater.* **2013**, *2* (10), 1370–1376.

(4) Kudgus, R. A.; Szabolcs, A.; Khan, J. A.; Walden, C. A.; Reid, J. M.; Robertson, J. D.; Bhattacharya, R.; Mukherjee, P. Inhibiting the growth of pancreatic adenocarcinoma in vitro and in vivo through targeted treatment with designer gold nanotherapeutics. *PloS One* **2013**, *8* (3), No. e57522.

(5) Jiang, S.; Win, K. Y.; Liu, S.; Teng, C. P.; Zheng, Y.; Han, M. Y. Surface-functionalized nanoparticles for biosensing and imaging-guided therapeutics. *Nanoscale* **2013**, *5* (8), 3127−3148.
(6) Chanana, M.; Rivera Gil, P.; Correa-Duarte, M. A.; Liz-Marzan, L. M.; Parak, W. J. Physicochemical properties of protein-coated gold nanoparticles in biological fluids and cells before and after proteolytic digestion. *Angew. Chem., Int. Ed.* **2013**, *52* (15), 4179−4183.
(7) Chikkaveeraiah, B. V.; Bhirde, A. A.; Morgan, N. Y.; Eden, H. S.; Chen, X. Electrochemical immunosensors for detection of cancer protein biomarkers. *ACS Nano* **2012**, *6* (8), 6546−6561.
(8) Szunerits, S.; Boukherroub, R. Sensing using localised surface plasmon resonance sensors. *Chem. Commun. (Cambridge, U. K.)* **2012**, *48* (72), 8999−9010.
(9) Nolan, J. P.; Duggan, E.; Liu, E.; Condello, D.; Dave, I.; Stoner, S. A. Single cell analysis using surface enhanced Raman scattering (SERS) tags. *Methods* **2012**, *57* (3), 272−279.
(10) Pan, D.; Mi, L.; Huang, Q.; Hu, J.; Fan, C. Genetic analysis with nanoPCR. *Integr. Biol.* **2012**, *4* (10), 1155−1163.
(11) Chen, X. J.; Sanchez-Gaytan, B. L.; Qian, Z.; Park, S. J. Noble metal nanoparticles in DNA detection and delivery. *Wiley Interdiscip. Rev.: Nanomed. Nanobiotechnol.* **2012**, *4* (3), 273−290.
(12) Kimling, J.; Maier, M.; Okenve, B.; Kotaidis, V.; Ballot, H.; Plech, A. Turkevich method for gold nanoparticle synthesis revisited. *J. Phys. Chem. B* **2006**, *110* (32), 15700−15707.
(13) Thakor, A. S.; Jokerst, J.; Zavaleta, C.; Massoud, T. F.; Gambhir, S. S. Gold nanoparticles: A revival in precious metal administration to patients. *Nano Lett.* **2011**, *11* (10), 4029−4036.
(14) Perrault, S. D.; Chan, W. C. Synthesis and surface modification of highly monodispersed, spherical gold nanoparticles of 50−200 nm. *J. Am. Chem. Soc.* **2009**, *131* (47), 17042−17043.
(15) Kim, J. H.; Kim, J. W. Simultaneously controlled directionality and valency on a water-soluble gold nanoparticle precursor for aqueous-phase anisotropic self-assembly. *Langmuir* **2010**, *26* (24), 18634−18638.
(16) Inbakandan, D.; Venkatesan, R.; Ajmal Khan, S. Biosynthesis of gold nanoparticles utilizing marine sponge *Acanthella elongata* (Dendy, 1905). *Colloids Surf., B* **2010**, *81* (2), 634−639.
(17) Kumar, S. S.; Kumar, C. S.; Mathiyarasu, J.; Phani, K. L. Stabilized gold nanoparticles by reduction using 3,4-ethylenedioxythiophene-polystyrenesulfonate in aqueous solutions: Nanocomposite formation, stability, and application in catalysis. *Langmuir* **2007**, *23* (6), 3401−3408.
(18) Botella, P.; Corma, A.; Navarro, M. T. Single gold nanoparticles encapsulated in monodispersed regular spheres of mesostructured silica produced by pseudomorphic transformation. *Chem. Mater.* **2007**, *19* (8), 1979−1983.
(19) Hwang, M. P.; Lee, J. W.; Lee, K. E.; Lee, K. H. Think modular: A simple apoferritin-based platform for the multifaceted detection of pancreatic cancer. *ACS Nano* **2013**, *7* (9), 8167−8174.
(20) Park, H.; Lee, J. W.; Hwang, M. P.; Lee, K. H. Quantification of cardiovascular disease biomarkers via functionalized magnetic beads and on-demand detachable quantum dots. *Nanoscale* **2013**, *5* (18), 8609−8615.
(21) Lee, K. H.; Galloway, J. F.; Park, J.; Dvoracek, C. M.; Dallas, M.; Konstantopoulos, K.; Maitra, A.; Searson, P. C. Quantitative molecular profiling of biomarkers for pancreatic cancer with functionalized quantum dots. *Nanomedicine* **2012**, *8* (7), 1043−1051.
(22) Aslam, M.; Fu, L.; Su, M.; Vijayamohanan, K.; Dravid, V. P. Novel one-step synthesis of amine-stabilized aqueous colloidal gold nanoparticles. *J. Mater. Chem.* **2004**, *14* (12), 1795−1797.
(23) Liu, X.; Atwater, M.; Wang, J.; Dai, Q.; Zou, J.; Brennan, J. P.; Huo, Q. A study on gold nanoparticle synthesis using oleylamine as both reducing agent and protecting ligand. *J. Nanosci. Nanotechnol.* **2007**, *7* (9), 3126−3133.
(24) Yang, Y.; Yan, Y.; Wang, W.; Li, J. Precise size control of hydrophobic gold nanoparticles using cooperative effect of refluxing ripening and seeding growth. *Nanotechnology* **2008**, *19* (17), 175603.